

Magnetic excitations in monodomain ferromagnetic uranium telluride

G. H. Lander

*Commission of the European Communities, Joint Research Centre, Institute for Transuranium Elements, Postfach 2340,
D-7500 Karlsruhe, Federal Republic of Germany*

W. G. Stirling

*Department of Physics, University of Keele, Keele, Staffordshire ST5 5BG, United Kingdom
and Science and Engineering Research Council, Daresbury Laboratory, Warrington WA4 4AD, United Kingdom*

J. M. Rossat-Mignod

*Département de Recherche Fondamentale, Service de Physique, Groupe de Magnétisme et Diffraction,
Centre d'Etudes Nucleaires, 85X, 38041 Grenoble, France*

M. Hagen

*Department of Physics, University of Keele, Keele, Staffordshire ST5 5BG, United Kingdom
and Neutron Division, Rutherford-Appleton Laboratory, Chilton, Oxon, United Kingdom*

O. Vogt

*Laboratorium für Festkörperphysik, Eidgenössische Technische Hochschule, CH-8093 Zürich, Switzerland
(Received 14 August 1989)*

Neutron-inelastic-scattering experiments have been performed with triple-axis spectrometers at the Institut Laue-Langevin, Grenoble, on a single-domain (field-cooled) crystal of the actinide ferromagnet ($T_c = 104$ K) UTe. The excitation at the zone center (Γ) has an anisotropy gap of 3.6 THz. In the direction of the easy axis $\langle 111 \rangle$, we are able to follow the excitation to the zone boundary, where the frequency is ~ 9 THz. In the perpendicular direction the excitation rapidly becomes strongly damped. This is the major new finding of our experiments on a single-domain crystal. The excitation is also broader than the resolution function throughout the zone. We have convoluted the instrumental Gaussian resolution function with a Lorentzian function to obtain this broadening quantitatively. A further broad "continuum" of magnetic scattering is also identified at low temperature; this contribution increases rapidly as the temperature is raised. Our measurements suggest that the $5f$ electrons in UTe strongly hybridize with the conduction electrons.

I. INTRODUCTION

The magnetic properties of the uranium monopnictides and monochalcogenides (all with the simple fcc NaCl crystal structure) have been of considerable interest since the first major attempt to explain their magnetic properties and electronic structure over 20 years ago.¹ All the compounds (denoted generically as UX) exhibit magnetic ordering, the pnictides being antiferromagnets, and the chalcogenides being ferromagnets. Early models for their electronic structure involved analogies with the lanthanide ($4f$) pnictides and chalcogenides and invoked crystal-field potentials acting on localized $5f$ electron states. Although the crystal-field potential is certainly important in these materials, and some models can make a reasonable attempt at explaining the magnetic properties,^{2,3} it is generally accepted that the $5f$ electrons strongly interact with their environment, thus making a localized $5f$ electron model inadequate. Apart from the results of neutron-scattering experiments, which we shall discuss in more detail below, the most persuasive evi-

dence that the properties of these systems require a complete treatment of not only the U $5f$ electrons but also their interaction with the $6d$ - $7s$ conduction band (all the systems are semimetallic in nature) comes from their transport properties⁴ and photoemission experiments.⁵ For example, in the case of uranium telluride, which is the subject of the present paper, the transport measurements of Schoenes *et al.*⁴ led them to conclude that UTe is a dense Kondo system with a very strong interaction between the $5f$ and band electrons and a rather large Kondo temperature. Similarly, the photoemission experiments of Reihl *et al.*⁵ were interpreted as showing a strong resonance occurring between the $5f$ electrons and the $6d$ band states.

In this paper we shall describe neutron-inelastic-scattering experiments to measure the magnetic response function of a monodomain sample of ferromagnetic UTe. The magnetic response function (or dynamical structure factor) $S(\mathbf{Q}, \omega)$ is a function of the momentum transfer \mathbf{Q} and the energy transfer $h\omega$ and also (implicitly) of temperature. This function is related directly to the imaginary part of the dynamic susceptibility, thus

$$S(\mathbf{Q}, \omega) = \frac{N}{\pi(g\mu_B)^2} [n(\omega) + 1] \\ \times \sum_{\alpha, \beta} (\delta_{\alpha\beta} - \mathbf{Q}_\alpha \mathbf{Q}_\beta / Q^2) \text{Im} X^{\alpha\beta}(\mathbf{Q}, \omega),$$

where $n(\omega) = (e^{h\omega/kT} - 1)^{-1}$ and gives the so-called detailed balance condition, the sum is over all components α, β in the magnetic system, and the term $(\delta_{\alpha\beta} - \mathbf{Q}_\alpha \mathbf{Q}_\beta / Q^2)$ ensures that scattering occurs from components perpendicular to \mathbf{Q} . The magnetic response functions of the UX compounds have been found to contain at least two major surprises. (A review of this work up to 1984 has been given by Buyers and Holden.⁶) The first is in the nature of the magnetic correlations that develop near the ordering temperature—the so-called critical regime. In the case of the antiferromagnets [see, for example, the work on UAs (Ref. 7), and also for a more recent study on a transuranium system PuSb (Ref. 8)], the unusual feature is the large anisotropy between the correlation lengths parallel and perpendicular to the ordering wave vector. Such anisotropies are not found in any other *cubic* systems, except for a few compounds containing cerium. In a series of papers Cooper and co-workers⁹⁻¹¹ have shown that this anisotropy arises from the nature of the anisotropic interactions between the *5f* and band electrons. Reasonable agreement is obtained between theory and experiment. In the case of the ferromagnets the multidomain nature of the sample above T_c and the fact that the ordering wave vector is $q = 0$ prevents the observation of this anisotropy in the critical regime. However, the ferromagnets show enormous magnetic anisotropy in their ordered state, which is a manifestation of the same interactions.

The second part of the $S(\mathbf{Q}, \omega)$ function that has been examined in detail, and especially since the first large crystals became available about twelve years ago, has been the low-temperature behavior of magnetic excitations. One would, of course, expect to see conventional magnetic excitations in all these materials because they order at reasonably high temperatures with appreciable magnetic moments. UTe, for example, orders at 104 K with an ordered moment of $2.25\mu_B$ per U atom.¹² Surprisingly, this is not the case. Well-defined propagating magnetic excitations are seen only in the case of the materials with a large lattice parameter, viz., USb (Refs. 2, 13, and 14) and UTe (Ref. 6), whereas for materials such as UN (Ref. 15), US (Ref. 16), and UAs (Ref. 17) only broad distributions of magnetic scattering, which have been interpreted as strongly overdamped spin waves, have been seen.

Uranium telluride (NaCl crystal structure, $a_0 = 6.16 \text{ \AA}$) has a $\langle 111 \rangle$ easy axis of magnetization and $T_c = 104 \text{ K}$. On ordering the material exhibits a rhombohedral distortion, which is a consequence of the magnetic moments being along the $\langle 111 \rangle$ body diagonal, and the resulting strain is 6.7×10^{-3} with the rhombohedral angle being 59.7° (60° in the cubic phase). The magnetization measurements of Busch *et al.*¹² show that the moment does not rotate from the easy $\langle 111 \rangle$ axis when an 8-T ap-

plied field is directed along either of the two other principal axes, $\langle 100 \rangle$ and $\langle 110 \rangle$. When a single crystal is cooled in zero field the moments will lie along any of the eight equivalent $\langle 111 \rangle$ directions, usually forming domains of equal population. Since we have stressed the giant magnetic anisotropy of these systems, it is likely that the magnetic response function is *different* for \mathbf{Q} parallel or perpendicular to the moment direction. Clearly, in a multidomain crystal such a separation is impossible to achieve.

Neutron-inelastic-scattering experiments on such a multidomain sample have been reported.⁶ At low temperatures (5 K), a sharp zone center (Γ point) magnetic excitation exists at an energy of $\sim 3.5 \text{ THz}$. This could be followed for only a very small distance [< 0.25 reciprocal lattice units (rlu)] away from Γ before being too broad to observe. This result suggests that UTe represents an interesting situation on the border between the reasonably localized behavior that can be assigned to USb (Refs. 2 and 14) and the strongly overdamped behavior of the other UX systems. In an effort to understand more completely the $S(\mathbf{Q}, \omega)$ function in the ordered state, we have performed experiments on a UTe crystal field-cooled to obtain a single domain. We then know precisely the moment direction μ , and can subsequently measure fluctuations with respect to this direction. We showed recently that this type of experiment, in that case on a monodomain sample of ferromagnetic PuSb,¹⁸ gave important information on the anisotropy in the magnetic excitation spectrum. A brief conference report of some of the measurements discussed here has been published.¹⁹

II. EXPERIMENTAL

All experiments were performed on the IN8 and IN20 triple-axis spectrometers at the Institut Laue-Langevin, Grenoble, France. The IN8 spectrometer (unpolarized neutrons) was used with focusing Cu(111) monochromator and pyrolytic graphite (002) analyzer with collimation $50'-40'-60'-60'$. The experiments were done with constant k_f scans with $k_f = 4.0$ or 4.2 \AA^{-1} , where k_f is the final neutron wave vector. Where appropriate, a pyrolytic graphite filter was used to suppress higher-order contamination.

One of the important experimental questions in UTe is whether there is any magnon interaction with the vibrational spectrum. The best method of separating magnetic from vibrational scattering is with polarized neutrons.²⁰ We have, therefore, attempted to do this using the IN20 triple-axis spectrometer with a Heusler alloy monochromator and analyzer. To separate magnetic and vibrational inelastic scattering²⁰ it is best to have the neutron-polarization axis parallel to the scattering vector \mathbf{Q} , which requires a horizontal field to produce a monodomain sample (see the following). The maximum field we were able to apply in this configuration was $\sim 1 \text{ T}$. This was sufficient to produce an almost monodomain sample, but, below T_c , we observed that the incident neutron beam was almost completely depolarized. Such an effect can arise from very small surface domains of the wrong polarity, and we believe these exist in our relative-

ly large UTe crystal despite the application of a field and field cooling this material. Thus the polarized-neutron experiments were not successful. All the experiments on IN8 and IN20 were therefore performed in an unpolarized mode with the same configuration, Cu(111) to PG(002).

The UTe crystal used in these measurements had a volume of $\sim 0.35 \text{ cm}^3$. For the experiments on IN8, it was mounted in a 10-T cryomagnet (constructed at the Centre d'Etudes Nucléaires de Grenoble), on a special holder which allowed rotation of the sample about a horizontal axis within the cryostat. The sample was cooled slowly through T_c with a 3-T magnetic field applied along the (vertical) $[1,1,1]$ axis to induce a monodomain state. At $T=5 \text{ K}$ the field was reduced to zero and the crystal was rotated by 90° about a $[1,-1,0]$ axis, perpendicular to the moment direction. The resulting horizontal scattering plane thus contains the moment direction μ , parallel to $[1,1,1]$, and the orthogonal $[1,-1,0]$ axis as shown in Fig. 1.

To simplify the following discussion, we denote the orthogonal axes of Fig. 1 as x ($[1,-1,0]$), y ($[1,1,-2]$), and z ($[1,1,1]$), and abbreviate the diagonal elements of $S^{\alpha\beta}(\mathbf{Q},\omega)$ as S^x ($=S^{xx}$), S^y ($=S^{yy}$), and S^z ($=S^{zz}$). To differentiate between the different components of the scattering function $S(\mathbf{Q},\omega)$ measured in different experimental configurations, we write the component of S corresponding to moment fluctuations in the x direction, with reduced propagation wave vector q_y , as $S^x q_y$, for example. We note that any off-diagonal elements, i.e., $S^{\alpha\beta}(\mathbf{Q},\omega)$ with $\alpha \neq \beta$, would not have been observable in the scans performed because the δ factor in the cross-section expression would be zero. This is a consequence of our experimental measurements being confined to the

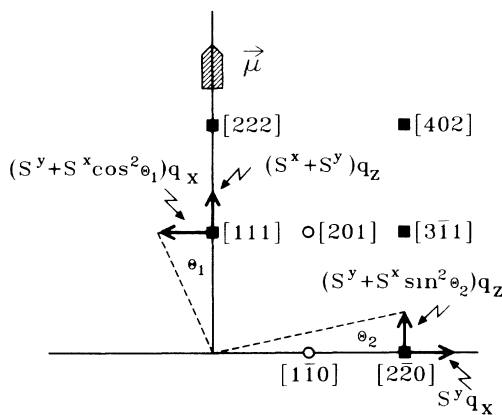


FIG. 1. Scattering plane used in UTe experiments. The moment direction $\mu \parallel [111]$. We call this the z axis. Perpendicular to this in the scattering plane is $[1\bar{1}0]$, which we call the x direction. The third orthogonal direction y is parallel to $[11\bar{2}]$ and perpendicular to the scattering plane. The components of $S(\mathbf{Q},\omega)$ that are measured around the $[111]$ and $[2\bar{2}0]$ Bragg points are marked. Zone centers are marked with a solid square.

high-symmetry directions, in this case z and x . For \mathbf{Q} in the z direction, $[1,1,1]$, we assume that there are no *longitudinal* moment fluctuations so that the components S^{zz} are identically zero. This is consistent with a relatively large ordered moment and the resulting polarization of the corresponding eigenstates. Magnetic neutron scattering measures only components of $S(\mathbf{Q},\omega)$ *perpendicular* to the scattering vector \mathbf{Q} . Thus, for example, for $\mathbf{Q}=(1.2,1.2,1.2)$, corresponding to a reduced wave vector $q_z=(0.2,0.2,0.2)$, the only components observable are $S^x q_z$ and $S^y q_z$, where these refer to components of S in the x or y direction for reduced wave vectors in the z direction.

III. RESULTS

A. Phonons

The magnetic excitations lie in the energy region $4 < E_M < 9 \text{ THz}$, whereas the optic-phonon branches, previously measured by Buyers and Holden,⁶ show relatively little dispersion about the energy $4.2 < E_{\text{ph}} < 4.7 \text{ THz}$. Although the phonon spectrum is normally independent

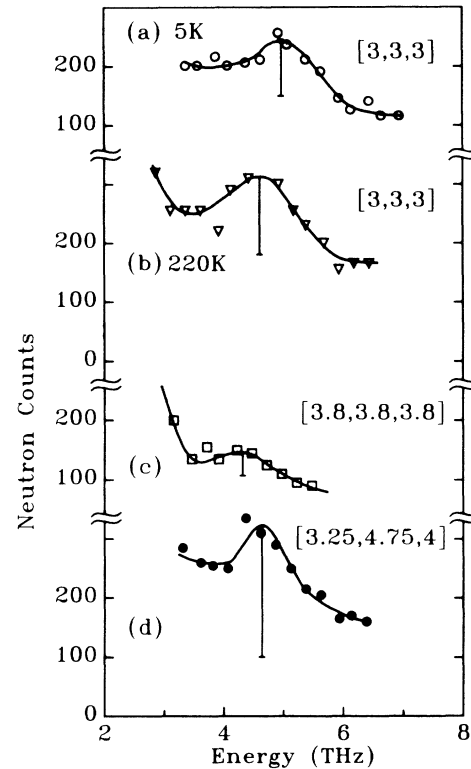


FIG. 2. Representative scans through optic phonons. In all cases, and in all subsequent figures, the vertical bar gives the calculated optic-phonon intensity. The horizontal position (energy) of the bar is taken from Ref. 6. (a) Zone center at $T=5 \text{ K}$; (b) zone center at $T=220 \text{ K}$; (c) longitudinal optic phonon at $q_z=0.2$ with small structure factor; (d) transverse optic phonon at $q_x=0.75$. The solid lines are Gaussian fits through the data points (IN8, monitor=3 K, $\sim 5 \text{ min/point}$).

of the magnetic-moment direction (except in the special case of magnon-phonon interaction), a determination of the magnetic excitation spectrum requires a detailed knowledge of the phonon dispersion curves, especially when the energy ranges overlap, as in the present case. The phonon frequencies determined in the present work on a (magnetic) monodomain sample are indeed in excellent agreement with the previous measurements. Since both optic phonons and magnetic excitations can contribute to the inelastic scattering observed at a particular wave vector, we have considered the optic-phonon intensities in some detail.

The phonon cross section is given by

$$I_{\phi}(\mathbf{q}, j) = [n(\omega) + 1] \sum_k \frac{b_k}{\sqrt{m_k}} |\mathbf{Q} \cdot \mathbf{e}(k, \mathbf{q}, j)|^2 e^{-W(\mathbf{Q})}$$

for mode j at reduced wave vector \mathbf{q} . The summation is made over atom types k , of mass m_k , and scattering length b_k . The mode eigenvector is $\mathbf{e}(k, \mathbf{q}, j)$ and $W(\mathbf{Q})$ is the Debye-Waller factor. Peckham²¹ has considered the inelastic structure factors of the isostructural compound MgO. In the present case of UTe, the fact that the ratios $b_{\text{U}}/(m_{\text{U}})^{1/2}$ and $b_{\text{Te}}/(m_{\text{Te}})^{1/2}$ are almost equal (0.055 and 0.048, respectively) leads to very small optic mode structure factors in “even” zones such as that centered on $(2, -2, 0)$. To estimate the optic-phonon contribution to the low-temperature inelastic scattering we have made high- Q phonon measurements at 220 K. Typical examples are shown in Fig. 2. All phonon peaks have the width expected from considerations of the instrumental resolution. From these data we have calculated the expected phonon intensity at all “magnetic” wave vectors and the resulting intensities are marked as vertical bars in subsequent figures or mentioned in the figure captions.

B. Magnetic scattering—low temperature

We show in Fig. 3 the magnetic excitation spectrum measured at the $(1, 1, 1)$ and $(2, -2, 0)$ reciprocal-lattice points. Since the moment is parallel to $(1, 1, 1)$ (see Fig. 1), these intensities should be related by a factor of 2, apart from the magnetic form factor, which can be written $f^2(Q) \approx \exp(-0.07Q^2)$. This is because we see $(S^x + S^y)q_z$ at the $(1, 1, 1)$ and $S^y q_z$ at $(2, -2, 0)$, both evaluated for $q_z = 0$. The vertical bar in Fig. 3(b) gives the expected magnetic intensity at the $(2, -2, 0)$ based on the $(1, 1, 1)$ intensity, and this is in good accord with the experiment. This scan, as well as others taken around the $(2, -2, 0)$, show that the sample is in a single-domain state. Furthermore, the good agreement between the intensities in Figs. 3(a) and 3(b) indicates that longitudinal fluctuations S^z are zero, or at least small.

We may then proceed to map the variation of the magnetic excitation spectrum as \mathbf{q} increases. In Fig. 4 we show scans at $q_z = 0.1, 0.2$, and 0.4 rlu (reciprocal-lattice units), as well as a constant energy scan at 6 THz. In this direction it is possible to measure the excitation across the whole zone (i.e., up to $q_z = 0.5$ rlu), although the peak width increases with q_z . We consider that the asymmetric peak shapes arise from effects of the vertical com-

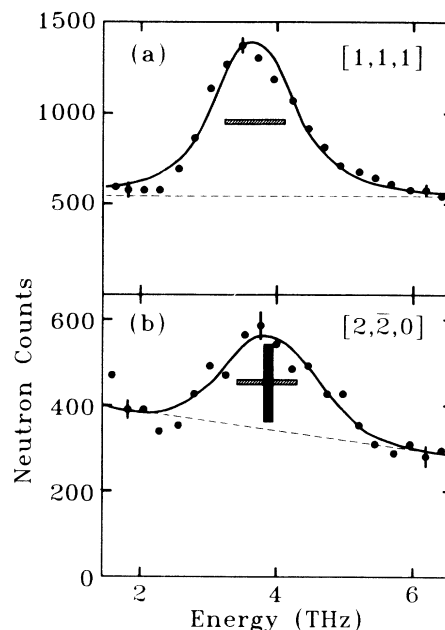


FIG. 3. Scans at $T = 5$ K at the (a) $(1, 1, 1)$ and (b) $(2, -2, 0)$ reciprocal-lattice points. The optic phonon contributes ~ 40 counts to scan (a) and less than 10 counts to scan (b). The solid lines in both (a) and (b) are the results of convoluting the experimental Gaussian resolution function of full width half maximum (FWHM) of 0.94 THz (horizontal bars) with a Lorentzian of FWHM = 0.84 THz. The vertical bar in (b) is the intensity expected at the $(2, -2, 0)$ position, based the $[111]$ intensity, if the sample is single domain. With no sample there are about 130 counts for the same monitor M (~ 18 min/point) (IN8, $M = 10$ K).

ponent of the instrumental resolution, combined with the mosaic structure of the sample. In the q_x direction the situation is more complex. In Fig. 5 we show scans at $q_x = 0.2, 0.4$, and 0.6 rlu, together with a constant E scan at 6.5 THz. The magnetic excitation spectrum is clearly more difficult to follow in this direction beyond $q_x = 0.4$ rlu. It seems likely that the intensity in Fig. 5(b) near 5 THz arises from the transverse optic phonon, although it may also have a magnetic contribution, with the main magnetic signal near 6.5 THz. This is borne out by the broad peak found in the constant E scan [Fig. 5(d)], which has the maximum signal centered at $q_x \sim 0.35$ rlu.

The complete dispersion relation of the magnetic excitation spectrum is plotted in Fig. 6. We may at this stage make a few remarks. First, the gap at Γ of $E_0 = 3.6 \pm 0.1$ THz (173 K) is in excellent agreement with previous work.⁶ This is to be expected as the anisotropy gap is clearly independent of whether the sample is single domain or not. However, in contrast to the work of Buyers and Holden,⁶ with a single-domain sample we are able to follow the dispersion curve to the zone boundary $q_z = 0.5$ (L point) in the $\langle 111 \rangle$ direction. Line broadening of ~ 0.8 THz is observed at the zone center (see Fig. 7) and this rises to ~ 2 THz towards the zone boundary, but there does not seem to be any direct interaction with

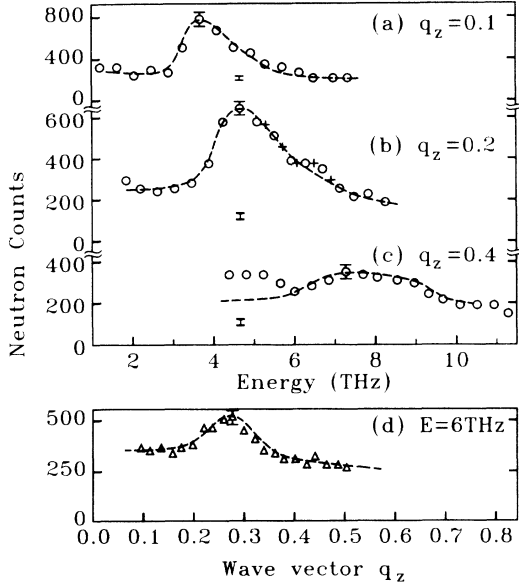


FIG. 4. Scans along q_z direction with (a) $q_z=0.1$; (b) $q_z=0.2$; (c) $q_z=0.4$; (d) constant energy ($E=6$ THz) as a function of q_z . The intensity of the optic phonons is marked as explained in Fig. 2. Scattering in (c) between 4 and 5 THz is from the sample holder. The lines are guides to the eye (IN8, $M=6$ K, ~ 11 min/point).

the optic phonon at $E=4.6$ THz. The excitation obeys the relationship $E=E_0+Dq^2$, with $E_0=3.6$ THz and $D=9.6\pm 1.0$ THz \AA^2 out to $q_z=0.4$ rlu (0.69 \AA^{-1}).

In the q_x direction, however, the excitation has almost the same dispersion as in the q_z direction up to $q_x \approx 0.35$ rlu. For $q_x \geq 0.4$ rlu, the excitation is difficult to observe. It is also possible that more than one excitation exists in this direction. Scattering appears at ~ 5 THz, which is stronger than the anticipated phonon signal, but in the absence of a clean separation with polarized neutrons we cannot be certain of this point.

In an attempt to quantify the line broadening we have convoluted the Gaussian resolution function of the instrument [FWHM (full width at half maximum)=0.94 THz] at an energy transfer of ~ 4 THz with a Lorentzian function to fit the experimental spectra (see Fig. 3 for zone-center fits), and the FWHM of these Lorentzian functions are plotted in Fig. 7. Significant line broadening is present even at the zone center and this increases as one moves across the zone.

C. Magnetic scattering—temperature dependence

The temperature dependence of the zone center and $q_z=0.2$ rlu excitations are shown in Figs. 8(a) and 8(b), respectively. Both excitations become broader with increasing temperature, and there is some renormalization of the zone-center mode.

In Fig. 9 we show (left-hand side) the variation of the relative intensity of the excitation as a function of temperature and (right-hand side) the temperature dependence of the relative energy gap (3.6 THz at 5 K). Al-

though we are unable to measure the energy gap above $T/T_c \sim 0.8$, it is clear that up to this reduced temperature it closely resembles the temperature variation of the magnetization.^{12,22} The variation of the energy gap with temperature appears to be somewhat different from that observed¹⁴ in USb. In that material the gap initially increases slightly before disappearing completely by $T/T_c \sim 0.75$, whereas in UTe we have been able to observe the gap to a slightly higher value of the reduced temperature.

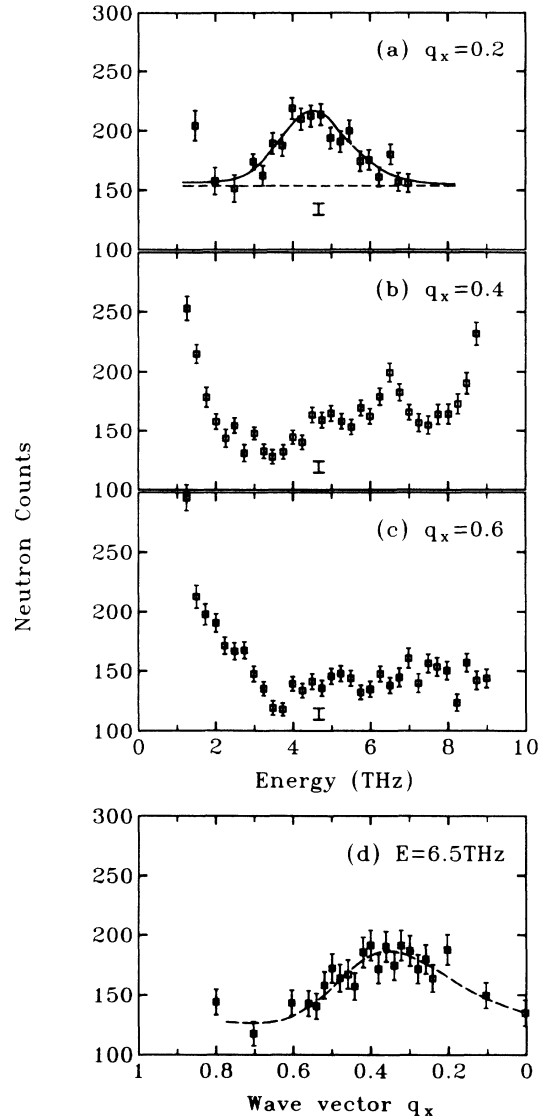


FIG. 5. Experimental scans along q_x direction with (a) $q_x=0.2$; (b) $q_x=0.4$; (c) $q_x=0.6$ rlu; (d) constant energy ($E=6.5$ THz) as a function of q_x . The increase in intensity at high-energy transfer is due to scattering from the incident neutron beam. The line in (a) corresponds to a fit as described in Fig. 3. Phonon intensities are indicated by vertical bars (IN20, $M=10$ K, ~ 8 min/point).

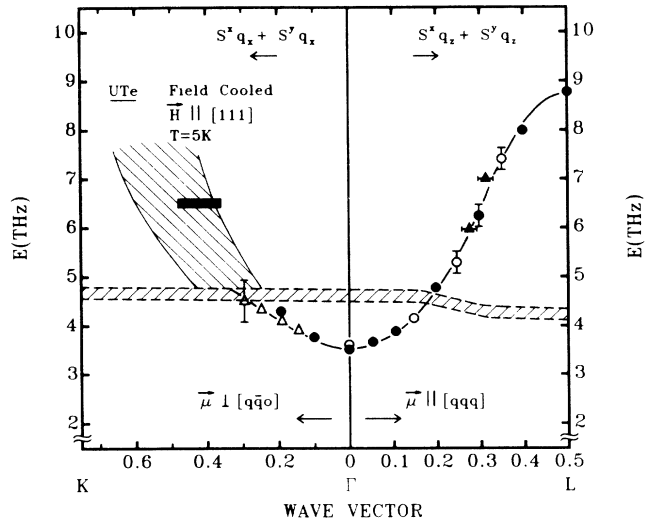


FIG. 6. Dispersion curve for UTe along the q_z (parallel to the moment) and q_x (perpendicular to the moment) directions at 5 K. The narrow hatched line shows the optic-phonon frequency. The different symbols correspond to different spectrometer conditions. The wide hatched area on the left-hand side corresponds to the region where we are unable to assign specific peak positions.

D. Observation of continuum magnetic scattering

The most distinctive part of the magnetic response in UTe at low temperature consists of spin-wave-like magnetic excitations over most of the zone. However, as

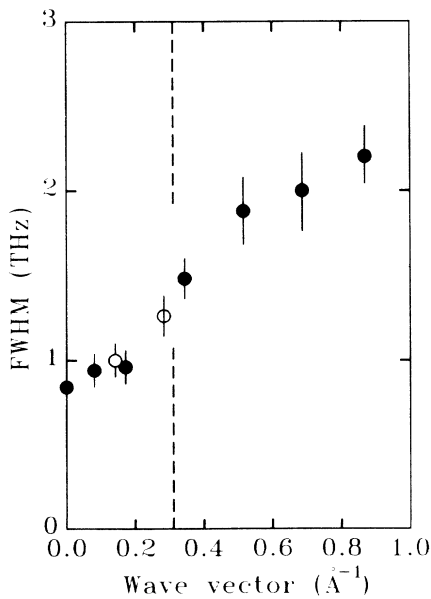


FIG. 7. FWHM of Lorentzian damping function at 5 K for excitation peaks as a function of q in \AA^{-1} . Solid points correspond to q_z , open points to q_x . The dashed vertical line indicates the wave vector at which the magnetic and optic-phonon excitation intersect.

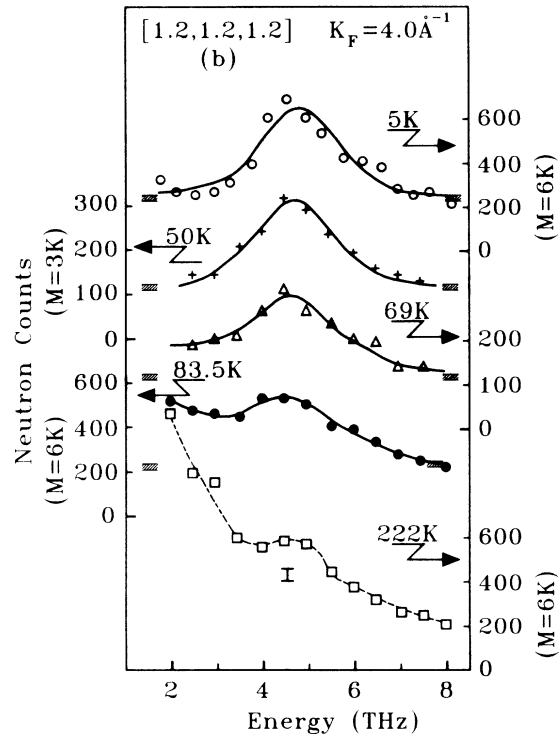
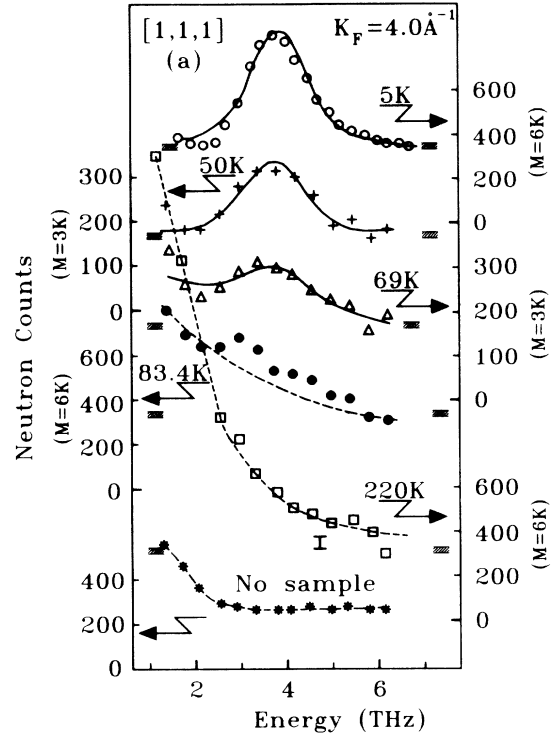


FIG. 8. Temperature dependence of the magnetic excitations at (a) $q_z=0$ and (b) $q_z=0.2$ rlu. Solid lines are fits as in Fig. 3, dashed lines are guides to the eye, and background levels are indicated by hatched bars (IN8).

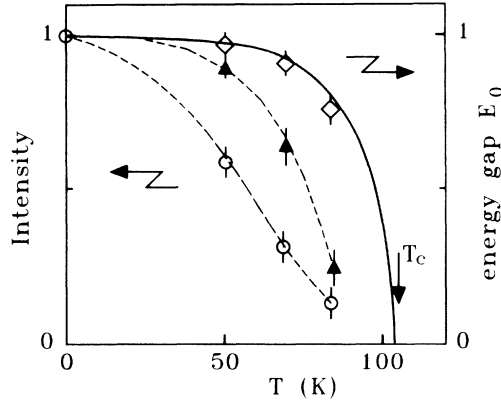


FIG. 9. Change of relative intensity of the zone center (open points) and $q_z = 0.2$ rlu (solid triangles) excitations as a function of temperature. For UTe, $T_c = 104 \pm 1$ K. Also plotted (diamonds) is the relative energy gap E_0 as a function of temperature as determined from the position of the excitation in Fig. 8. The Bose factors, which are within 10% of unity, have been removed in making these comparisons. The lines are guides to the eye except for the solid curve, which is the variation of the magnetic moment as measured by magnetization on a single crystal (Ref. 12).

shown in Fig. 7 these spin waves do not exhibit the instrumental resolution so that a broadening mechanism, presumably as a result of interaction with the conduction electrons, must be invoked. In the course of our experiment we have also observed an additional feature that we characterize as a continuum of magnetic scattering. This aspect of the $S(\mathbf{Q}, \omega)$ response has a relatively weak q dependence and is much smaller at low temperature. The abrupt rise of the scattering at low-energy transfer as a function of temperature may be seen from Fig. 8. It seems reasonable to suppose this scattering is coupled to the broadening of the spin waves even at Γ in UTe at low temperature. For example, such continuum scattering has been found absent in USb at 5 K and in this material the spin waves are resolution limited at low temperature.¹⁴ Similarly, such continuum scattering has been identified in both UN (Ref. 15) and US (Ref. 16) in which the spin waves are strongly overdamped and essentially unobservable.

It is well known that a triple-axis spectrometer with its good resolution in q space is not the best instrument with which to examine this broad magnetic response function. A better way is with a time-of-flight instrument on a polycrystalline sample, although much of the q dependence is then lost. Such experiments have been performed at the Rutherford Appleton Laboratory (U.K.) spallation source ISIS, and a preliminary account²³ of the low-temperature results on UTe has been published. In excellent agreement with the present study, these authors find evidence for a “tail” of magnetic scattering extending in energy from the spin-wave band up to approximately 20–25 THz.

IV. DISCUSSION

Our present experiments on a monodomain sample of UTe have shown that the dispersion relationship is anisotropic with less dispersion and more damping in the direction transverse to the moment than in the direction parallel to the moment. To our knowledge, such anisotropy is most unusual in *cubic* ferromagnets and has only been observed previously in PuSb.¹⁸

We may describe this anisotropy in terms of the imaginary part of the magnetic susceptibility, which is what is measured in the neutron-inelastic-scattering experiment. Thus, the excitations represented as $S^x q_z$ and $S^y q_z$ arise from the expressions $\text{Im}X^{xx}(0, 0, q_z)$ and $\text{Im}X^{yy}(0, 0, q_z)$, respectively. These are related to the ferromagnetic coupling within the plane perpendicular to the moment direction. The excitations represented as $S^x q_x$ and $S^y q_x$ arise from the expressions $\text{Im}X^{xx}(q_x, 0, 0)$ and $\text{Im}X^{yy}(q_x, 0, 0)$, respectively. These are *not* equivalent by symmetry, nor are they necessarily equivalent to $\text{Im}X^{xx}(0, 0, q_z)$, and are related to the strength of the ferromagnetic exchange interactions along the direction of the magnetic moment. The fact that $\text{Im}X^{xx}(q_x, 0, 0)$ is not equivalent to $\text{Im}X^{yy}(q_x, 0, 0)$ means that more than one excitation may be present in the q_x direction. This has been observed directly in PuSb.¹⁸ However, the splitting of the modes, which are always resolution limited in PuSb, occurs near the zone boundary. In the case of UTe we have not been able to observe the excitation further than $q_x = 0.5$ rlu, but it may well be that by this point the mode has split into two broad peaks that are too weak to be observed.

The phonon dispersion curves for UTe are discussed in Ref. 6. They show an anomaly, especially in the [111] direction, in which the longitudinal modes, both acoustic and optic, have lower frequencies at the zone boundary than the transverse modes. Furthermore, c_{12} and Poisson’s ratio are negative for UTe and the bulk modulus is anomalously low.²⁴ These anomalies have been discussed in terms of either a large Kondo temperature⁴ or a mixed valence state; however, a quantitative understanding of these properties is still lacking. In the present experiment one of our objectives was to search for any interaction of magnetic excitations with the optic phonons, see Fig. 6. We have not found evidence for such an interaction. For wave vectors q_z , the damping (Fig. 7) is a function of the magnitude of q_z rather than being associated with the frequency of the optic phonons. For wave vectors q_x , the magnetic excitation does indeed appear to decrease in intensity when it reaches ~ 5 THz, and we cannot exclude a magnon-phonon interaction. Unfortunately, our efforts to examine this directly with polarized neutrons were unsuccessful because of the neutron depolarization effects discussed earlier.

The theoretical treatments of Cooper and co-workers,^{9–11} developed for cerium compounds, have recently been extended to consider the excitation behavior of the actinide rocksalt compounds. In discussing the excitations in the ferromagnetic PuSb they showed²⁵ that the anomalous behavior at the zone boundary¹⁸ could be explained as a consequence of the strong anisotropic in-

teraction between the almost localized $5f$ electrons in PuSb and the band electrons. For PuSb the spectral weight and distribution is changed as a result of the hybridization, but there is very little damping of the excitations. In the experiment, at least at $T=0$, we also observe no damping of the excitation. The theoretical situation is more complex for the UX materials; this is a consequence both of the greater hybridization of $5f$ electrons and of the larger number of conduction electrons (Pu $5f^5$ may be treated as a single-hole problem). In their first report the authors²⁶ have treated UP and UAs and have shown that, in agreement with experiment, broad rather than well-defined excitation spectra are obtained as a consequence of both the (anisotropic) two-ion hybridization-mediated interactions and of the increase of the single-site hybridization parameter (as compared to Ce and Pu). As a result of our experimental investigations, Hu and Cooper,²⁷ have now specifically treated UTe. In excellent agreement with our results they find the following: (a) the excitation is well defined in the q_z direction, and (b) in the q_x direction at moderate wave vectors more than one excitation should be observed. The consequences of the damping and finite instrumental resolution make it difficult to distinguish between a single damped excitation and more than one excitation.

In conclusion, our studies of UTe have indeed shown that the $5f$ electrons in UTe are strongly hybridized with the conduction electrons. The interaction between the $5f$ electrons and the conduction electron band sea can be clearly seen in both the damping of the excitations, even at the zone center, and the diffuse magnetic response function. These observations can be understood on the basis of the detailed theory developed by Hu and Cooper.²⁷ Such agreement portends a significant advance in our understanding of the many other physical properties, for example the transport properties⁴ and photoemission results,⁵ which have been reported about the intriguing series of UX compounds.

ACKNOWLEDGMENTS

The measurements reported here were performed at the Institut Laue-Langevin, Grenoble, France. Many people at that Institute and at the Centre d'Etudes Nucléaires Grenoble assisted us; in particular, we wish to thank M. Alba, A. Brochier, J. Olivier, A. Severing, and C. Vettier. We thank K. Mattenberger for assistance in the crystal growth and B. R. Cooper for a number of stimulating discussions.

- ¹J. Grünzweig-Genossar, M. Kuznietz, and F. Friedman, *Phys. Rev.* **173**, 562 (1968).
- ²B. Halg and A. Furrer, *Phys. Rev. B* **34**, 6258 (1986).
- ³T. M. Holden, J. A. Jackman, W. J. L. Buyers, K. M. Hughes, M. F. Collins, P. de V. Du Plessis, and O. Vogt, *J. Magn. Magn. Mater.* **63-64**, 155 (1987).
- ⁴J. Schoenes, B. Frick, and O. Vogt, *Phys. Rev. B* **30**, 6578 (1984).
- ⁵B. Reihl, N. Martensson, P. Heimann, D. E. Eastman, and O. Vogt, *Phys. Rev. Lett.* **46**, 1480 (1981).
- ⁶W. J. L. Buyers and T. M. Holden, in *Handbook of the Physics and Chemistry of the Actinides*, edited by A. J. Freeman and G. H. Lander (North-Holland, Amsterdam, 1985), Vol. 2, p. 239.
- ⁷S. K. Sinha, G. H. Lander, S. M. Shapiro, and O. Vogt, *Phys. Rev. B* **23**, 4556 (1981), and references therein; see also B. Halg and A. Furrer, *J. Appl. Phys.* **55**, 1860 (1984).
- ⁸P. Burllet, J. Rossat-Mignod, G. H. Lander, J. C. Spirlet, J. Rebizant, and O. Vogt, *Phys. Rev. B* **36**, 5306 (1987).
- ⁹B. R. Cooper, R. Siemann, D. Yang, P. Thayamballi, and A. Banerjea, in *Handbook of the Physics and Chemistry of Actinides*, edited by A. J. Freeman and G. H. Lander (North-Holland, Amsterdam, 1985), Vol. 2, p. 435.
- ¹⁰J. M. Wills and B. R. Cooper, *Phys. Rev. B* **36**, 3809 (1987).
- ¹¹N. Kioussis, B. R. Cooper, and A. Banerjea, *Phys. Rev. B* **38**, 9132 (1988).
- ¹²G. Busch, O. Vogt, A. Delapalme, and G. H. Lander, *J. Phys. C* **12**, 1391 (1979).
- ¹³G. H. Lander, W. G. Stirling, and O. Vogt, *Phys. Rev. Lett.* **42**, 260 (1979); G. H. Lander and W. G. Stirling, *Phys. Rev. B* **21**, 436 (1980).
- ¹⁴M. Hagen, W. G. Stirling, and G. H. Lander, *Phys. Rev. B* **37**, 1846 (1988).
- ¹⁵T. M. Holden, W. J. L. Buyers, E. C. Svensson, and G. H. Lander, *Phys. Rev. B* **30**, 114 (1984).
- ¹⁶T. M. Holden, W. J. L. Buyers, P. de V. Du Plessis, K. M. Hughes, and M. F. Collins, *J. Magn. Magn. Mater.* **54-57**, 1175 (1986).
- ¹⁷W. G. Stirling, G. H. Lander, and O. Vogt, *Physica* **102B**, 249 (1980); M. Loewenhaupt, G. H. Lander, A. P. Murani, and A. Murasik, *J. Phys. C* **15**, 6199 (1982).
- ¹⁸G. H. Lander, W. G. Stirling, J. Rossat-Mignod, J. C. Spirlet, J. Rebizant, and O. Vogt, *Physica* **136B**, 409 (1986).
- ¹⁹G. H. Lander, W. G. Stirling, J. M. Rossat-Mignod, M. Hagen, and O. Vogt, *Physica* **156-157B**, 826 (1989).
- ²⁰R. M. Moon, T. Riste, and W. C. Koehler, *Phys. Rev.* **181**, 920 (1969).
- ²¹G. Peckham, *Proc. Phys. Soc. London* **90**, 657 (1967).
- ²²A. T. Aldred, P. de V. Du Plessis, and G. H. Lander, *J. Magn. Magn. Mater.* **20**, 236 (1980).
- ²³R. Osborn, M. Hagen, D. L. Jones, W. G. Stirling, G. H. Lander, K. Mattenberger, and O. Vogt, *J. Magn. Magn. Mater.* **76-77**, 429 (1988).
- ²⁴J. M. Leger, I. Vedel, A. M. Redon, J. Rossat-Mignod, and O. Vogt, *Solid State Commun.* **66**, 1173 (1988).
- ²⁵G. J. Hu, N. Kioussis, A. Banerjea, and B. R. Cooper, *Phys. Rev. B* **38**, 2639 (1988).
- ²⁶G. J. Hu, B. R. Cooper, and G. H. Lander, *Physica* **156-157B**, 822 (1989).
- ²⁷G. J. Hu and B. R. Cooper (unpublished).